Advanced two-stage cascade configurations for energy-efficient –80 °C refrigeration

Cosmin-Mihai Udroiu, Adrián Mota-Babiloni*, Joaquín Navarro-Esbrí

ISTENER Research Group, Department of Mechanical Engineering and Construction, Universitat Jaume I, Castelló de la Plana, E-12071, Spain

Abstract

In response to the COVID-19 pandemic, some vaccines have been developed requiring ultralow-temperature refrigeration, and the number of these freezers has been increased worldwide. Ultralow-temperature refrigeration operates with a significant temperature lift and, hence, a massive decrease in energy performance. Therefore, cascade cycles based on two vapor compression single-stage cycles are traditionally used for these temperatures. This paper proposes the combination of six different cycles (single-stage with and without internal heat exchanger, vapor injection, liquid injection, and parallel compression with and without economizer) in two-stage cascades to analyze the operational and energetic performance in ultralow-temperature freezers. All this leads to 42 different configurations in which the intermediate cascade temperature is optimized to maximize the coefficient of performance. Ultra-low global warming potential natural refrigerants such as R-290 (propane) and R-170 (ethane) for the cascade high- and low-stage have been considered. From the thermodynamic analysis, it can be concluded that liquid and vapor injection cascade configurations are the most energy-efficient. More specifically, those containing a vapor injection in the low-temperature stage (0.89 coefficient of performance, 40 % higher than traditional configurations). Then, using an internal heat exchanger for such low temperatures is unnecessary in terms of performance. The optimum intermediate cascade temperature varies significantly among cycles, from -37 to 2 °C, substantially impacting energy performance. Parallel compression configuration improves energy performance over single-stage cycles, but not as much as multi-stage (between 20 % and 30 % lower coefficient of performance). It can be seen as the high-temperature stage can be based on a single-stage cycle while keeping the maximum coefficient of performance observed with vapor injection in the low-temperature stage.

Keywords: ultralow-temperature refrigeration; cascade; multi-stage configurations; parallel compression; coefficient of performance (COP); natural refrigerants.

Nomenclature

$\dot{m}$	Refrigerant mass flow rate (kg s^{-1})
$\dot{Q}$	Heat transfer (kW)
h	Enthalpy (kJ kg^{-1})
P	Pressure (MPa)

* Corresponding author: Adrián Mota Babiloni,PhD
e-mail: mota@uji.es Phone: +34 964 728 134

$\dot{W}$	Power consumption (kW)
T	Temperature (K)
S	Single-stage cycle
I	Single-stage cycle with internal heat exchanger
L	Two-stage cycle with liquid injection
V	Two-stage cycle with vapor injection
P	Parallel compression
E	Parallel compression with economizer

Greek symbols

η	Efficiency (-)
Δ	Variation (-)

Subscripts

ref	Refrigerant
$evap$	Evaporator
il	Intermediate line
in	Inlet
out	Outlet
iso	Isentropic
suc	Suction
$disc$	Discharge
$comp$	Compressor
hot	Hot fluid
$cold$	Cold fluid
I	Intermediate
HT	High temperature
LT	Low temperature
e	Equivalent

Abbreviations

COP	Coefficient of performance
HFC	Hydrofluorocarbon
GWP	AR5 100-yr global warming potential
LT	Low-temperature
HT	High-temperature
CR	Compression ratio
IHX	Internal heat exchanger
BF	Bypass factor

1. Introduction

Ultralow-temperature refrigeration consists of cooling a particular product or room below a specific temperature, generally below –50 ºC [1]. The recent appearance of the Sars-CoV-2 vaccines has put the light on a problem that has been present in society for a long time, deep freezing. Pfizer-BioNTech announced that its vaccines must be stored between –60 ºC and –80

ºC [2]. Consequently, news reports have echoed, alleging a huge logistical problem to keep vaccines in such conditions.

Refrigeration at this temperature range is usually based on vapor compression systems. There is a lack of studies and regulations in the ultralow-temperature range to motivate advanced environmentally-friendly solutions [3]. The impact of energy efficiency on equivalent carbon dioxide emissions requires studying the broadest combination of configurations in detail. Cascade and auto-cascade systems are configurations typically found in commercial low or ultralow-temperature freezers [4], working between 20 and 30 °C ambient temperature and –50 to –80 °C freezing conditions [5].

The cascade configuration thermally connects single-stage cycles through a cascade heat exchanger, choosing the most suitable refrigerant for each temperature level. Most of the available studies for this application consider only two stages [6]. Compared to a two-stage configuration, Mumanachit et al. [7] observed that a two-stage cascade is more efficient below the coefficient of performance (COP) optimal point and cost-effective below –46.2 ºC. Mateu-Royo et al. [8] observed that a two-stage cascade becomes the most appropriate configuration for high temperature lifts (60 K and above).

Furthermore, controlling the operational characteristics of two-stage cascades is essential for proper energy performance. Chung et al. [9] observed that a higher low-temperature (LT) compressor discharge pressure allows a lower evaporator temperature. In addition, an inadequate pressure adjustment can cause fluctuations in the compressor operation and the cascade temperature distribution. Lee et al. [10] concluded that the COP increases with increasing LT evaporation temperature but decreases with increasing high-temperature (HT) condensation temperature and temperature variation. Chae and Choi [11] showed that the COP is lower when the system is undercharged because the heat transfer capacity decreases. Deymi-Dashtebayaz et al. [12] proposed the Pareto front curve to obtain the optimal operational conditions and refrigerants considering maximum COP, maximum exergy efficiency and minimum total cost rate. R-41/R-161 and R-41/R-1234ze(E) present the highest COP and exergy efficiency and lowest total cost rate.

Cascade configurations based on single stages can be modified by adding elements such as the internal heat exchanger (IHX, also known as liquid-to-suction heat exchanger). Di Nicola et al. [13] proposed an IHX in the LT stage, concluding that it could be helpful. Bhattacharyya et al. [14] optimized a cascade system with IHX in HT and LT stages and observed that the system performance does not depend on the IHX effectiveness. Liu et al. [15] concluded that the COP is lower if only the LT IHX operates, but the cycle with IHX in both stages has the potential to be energy efficient. Also, Dubey et al. [16] observed that the HT IHX impact on system performance is higher than that of the LT stage.

Although it challenges the design and control, cascades in ultralow-temperature refrigeration are not limited to two stages and can be composed of three or more stages. Agnew and Ameli [17] studied a three-stage cascade, but they did not provide practical conclusions. Johnson et al. [18] developed a three-stage cascade with dynamic control, showing effectiveness against flow

disturbances in the secondary fluid. Sun et al. [19] compared several refrigerants in each stage of a three-stage cascade, and they recommended the following groups of refrigerants: R-1150/R-41/R-717, R-1150/R-41/R-152a, R-1150/R-41/R-161, R-1150/R-170/R-717, R-1150/R-170/R-152a, and R-1150/R-170/R-161. Walid Faruque et al. [20] determined that at −120 and −110 °C evaporation temperature, 1-butene/Heptane/m-Xylene combination results in the maximum performance, while 1-butene/Toluene/m-Xylene combination at −100 and −90 °C evaporation temperature.

Due to the greenhouse effect caused by traditional refrigerants, the European Union approved the (F-Gas) Regulation 517/2014 [21], which aims to reduce refrigerants' equivalent carbon dioxide emissions by two-thirds in 2030 compared to 2014 levels. Scientific articles published about refrigerants show that studying environmentally friendly refrigerants in cascades is essential.

Many previous studies considered ammonia (R-717) and carbon dioxide (R-744) for low temperature refrigeration (down to –40 ºC evaporation temperature). Dopazo et al. [22] quantified with R-744 and R-717 that an increase in the evaporator temperature from –55 ºC to –30 ºC leads to a 70 % higher COP. In the same way, an increase in the condenser temperature from 25 ºC to 50 ºC causes a 45 % lower COP. Additionally, if the cascade heat exchanger temperature increases from 3 ºC to 6 ºC, it causes a 9 % COP reduction. Di Nicola et al. [13] compared different hydrofluorocarbons (HFCs) with R-717 at –70 ºC, concluding that the latest is 5 % superior in COP. Getu and Bansal [23] found with R-744 and R-717 refrigerants that a higher superheating degree and mass flow ratio decreases the COP. Still, it can be counteracted with higher subcooling in both stages. Eini et al. [24] compared R-744/R-717 and R-744/R-290 pairs, concluding that the one with R-717 is inherent safety. Ust and Karakurt [25] concluded that R-717 in the HT stage causes higher energy performance than R-290, R-404A, and R-507. Turgut and Turgut [26] tested the refrigerant pairs R-744/R-717, R-744/R-134a, and R-744/R-1234yf, observing that R-744/R-1234yf is superior as regards efficiency and annual costs. On the other hand, subcooling and superheating degrees have a negligible influence on the cost of the equipment.

According to Sun et al. [27], an optimal cascade heat exchanger temperature is essential, and R-41 is appropriate to replace R-23. Kilicarslan and Hosoz [28] expanded the selection of refrigerants by proposing R-152a/R-23, R-290/R-23, R-507/R-23, R-134a/R-23, R-717/R-23, and R-404A/R-23 to assess the influence of the operating temperature on the COP. Aktemur et al. [29] considered other novel refrigerants such as R-1243zf, R-423A, R-601, R-601a, R-1233zd(E) and RE-170, concluding that R-432A shows the lowest energy performance. Mota-Babiloni et al. [30] found significant differences in the selection of the LT and HT refrigerants for high temperature heat pumps, regarding COP and volumetric heating capacity, even with optimized cascade intermediate temperature.

Regarding lower evaporating temperatures, Adebayo et al. [31] concluded that R-717/R-744 results in the highest COP at –50 ºC in evaporation, while the lowest is HFE-7100/R-744, being R-134a and HFE-7000 in an intermediate position. Rodríguez-Criado et al. [32] adapted a

standard low-temperature R-290 packaged unit with R-170 between –80 °C and –65 °C of evaporating temperature, and they measured between 0.6 and 1.6 COP.

The literature shows that cascade systems at ultralow temperatures have hardly been studied. Only a few works propose the incorporation of IHXs, but there are more possibilities to modify single-stage cycles composing cascade configurations and enhance overall energy performance. Moreover, few works consider the refrigerant pair R-290/R-170, which can be the most promising in terms of energy performance and global warming contribution. Most papers dealing with cascade configurations hardly reach the extreme evaporation temperature of -80°C. Because of the recent interest in this application and the evident lack of studies, this work proposes the combination of different vapor compression cycles in cascade configurations. Firstly, the way to combine cycles and construct configurations is presented. Next, the methods and strategy of the simulation, including equations and input parameters, the behavior of cycles, and refrigerants, are exposed. Then, the computational simulation results are analyzed and discussed, focusing on COP, optimum intermediate temperature, and mass flow rate. Finally, the main conclusions of the study are summarized.

2. Methods

The methods will explain the configurations used from the standard vapor compression cycles to the cascade ones. A strategy has been used from the assumptions to the final modeling details.

2.1. Configurations

This article combines six standard vapor compression cycles in the high and low-temperature stages of a cascade configuration. As ultralow-temperature applications must cover a significantly high-temperature lift (difference between condensation and evaporation temperatures), cascade configurations could benefit from improvement in stages. Therefore, all possible combinations are simulated in the same operating point, and the energetic efficiency is assessed. These cycles that are combined in the paper are shown in Figure 1.

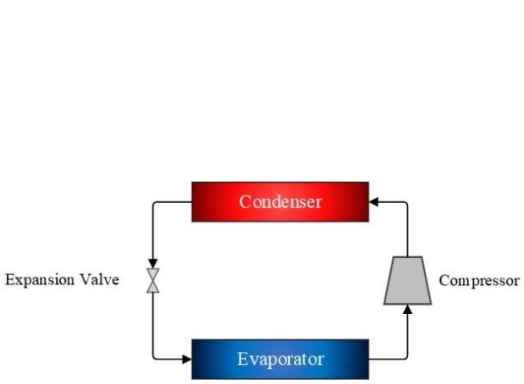

Single-stage cycle

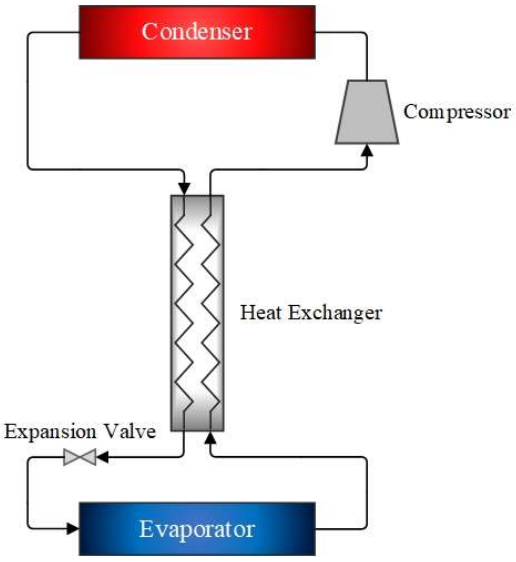

Single-stage cycle with internal heat

exchanger

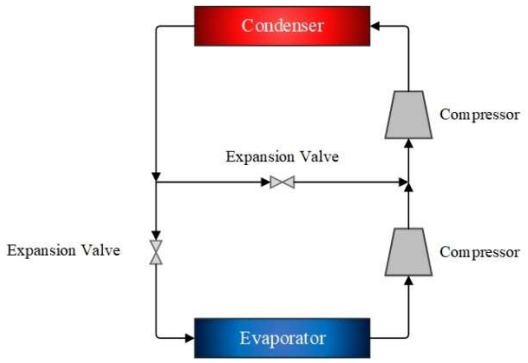

Two-stage cycle with liquid injection

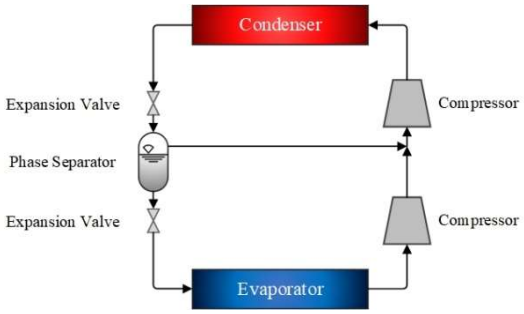

Two-stage cycle with vapor injection

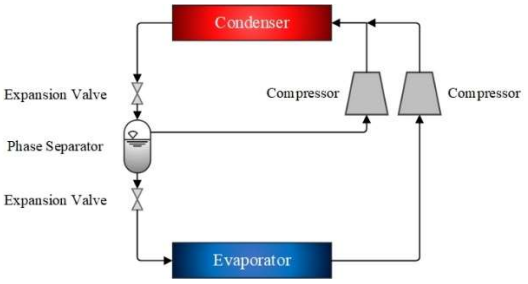

Parallel compression

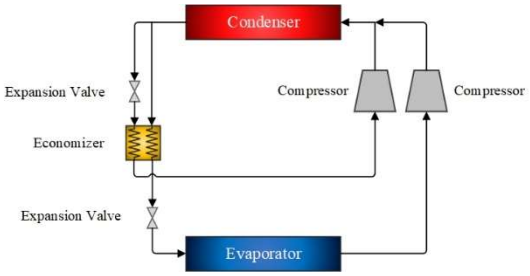

Parallel compression with economizer

Figure 1. Schematic of cycles combined in cascade.

A total of 42 configurations are defined, considering these cycles in both possible cascade stages. Table 1 describes all configurations simulated in this paper and the abbreviature proposed for simplifying the analysis process.

Table 1. List of configurations studied in this paper.

HT	**LT**	**Abbreviature**
Single-stage cycle		S
Single-stage cycle with IHX		I
Two-stage cycle with liquid injection		L
Two-stage cycle with vapor injection		V
Parallel compression		P
Parallel compression with economizer		E
Single-stage	Single-stage	S+S

Single-stage with IHX	Single-stage with IHX	I+I
Single-stage with IHX	Single-stage	I+S
Single-stage	Single-stage with IHX	S+I
Liquid injection	Liquid injection	L+L
Liquid injection	Single-stage	L+S
Single-stage	Liquid injection	S+L
Liquid injection	Single-stage with IHX	L+I
Single-stage with IHX	Liquid injection	I+L
Vapor injection	Vapor injection	V+V
Vapor injection	Single-stage	V+S
Vapor injection	Single-stage with IHX	V+I
Single-stage	Vapor injection	S+V
Single-stage with IHX	Vapor injection	I+V
Vapor injection	Liquid injection	V+L
Liquid injection	Vapor injection	L+V
Parallel compression	Parallel compression	P+P
Parallel compression with economizer	Parallel compression with economizer	E+E
Parallel compression	Single-stage	P+S
Parallel compression	Single-stage with IHX	P+I
Single-stage	Parallel compression	S+P
Single-stage with IHX	Parallel compression	I+P
Parallel compression	Liquid injection	P+L
Liquid injection	Parallel compression	L+P
Parallel compression	Vapor injection	P+V
Vapor injection	Parallel compression	V+P
Parallel compression with economizer	Single-stage	E+S
Parallel compression with economizer	Single-stage with IHX	E+I
Single-stage	Parallel compression with economizer	S+E
Single-stage with IHX	Parallel compression with economizer	I+E
Parallel compression with economizer	Liquid injection	E+L
Liquid injection	Parallel compression with economizer	L+E
Parallel compression with economizer	Vapor injection	E+V
Vapor injection	Parallel compression with economizer	V+E
Parallel compression	Parallel compression with economizer	P+E
Parallel compression with economizer	Parallel compression	E+P

Figure 2 illustrates the configuration of a two-stage cascade based on two single-stage cycles (S+S). These configurations will be used as a baseline, and other configurations will replace single stages to achieve the maximum number of possible combinations. The intermediate temperature is decisive in the system energy performance, among other factors.

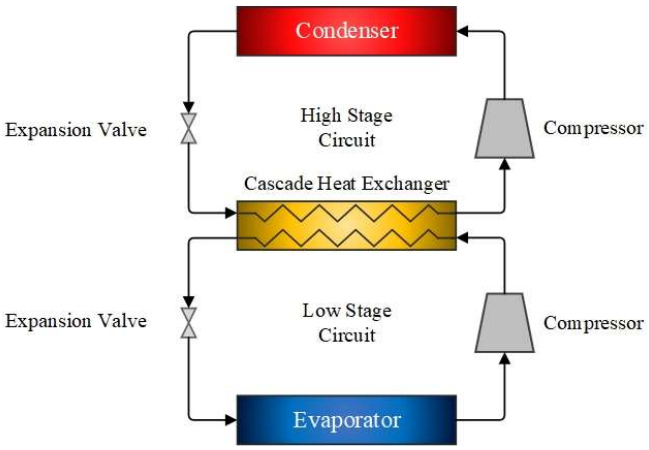

Figure 2. Schematic of a two-stage cascade.

The configurations explained above have been calculated with the following strategy.

2.2. Strategy

The simulation of the configurations is based on the methods presented in Figure 3, where the input parameters are configuration, refrigerants, and boundary conditions and assumptions. This model is developed using the software Engineering Equation Solver (EES) [33] version Academic Commercial V100.835-3D. The Golden Search Algorithm incorporated in this software is used to find the optimum cascade heat exchanger temperature that maximizes COP.

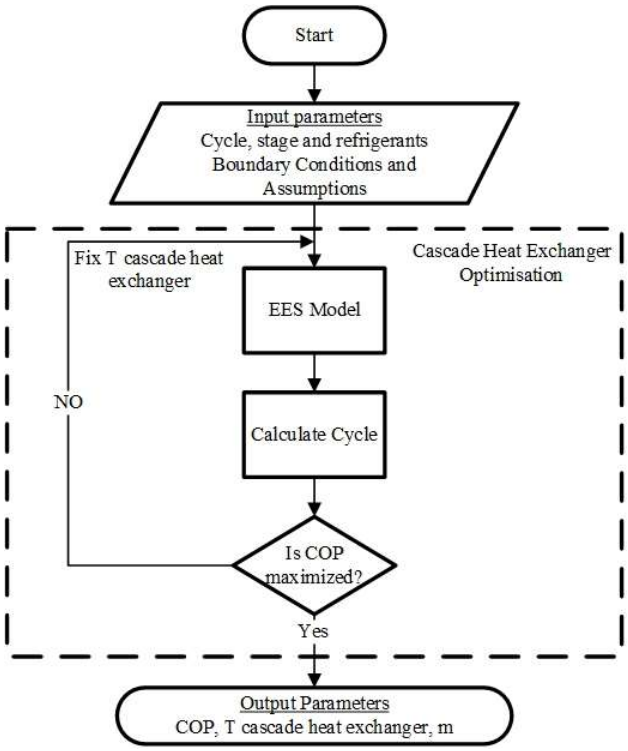

Figure 3. Methods flow diagram.

Other information required for the modeling is exposed in the following subsections.

2.3. Boundary conditions and assumptions

The input parameters used in calculating the cycles are shown in Table 2. Evaporating temperature is set at the typical minimum value of ultralow-temperature freezers, even though they can work from −50 °C. Hence, this temperature was selected for the study to cover the most critical condition. Then, the condensing temperature of 30 °C was chosen to simulate controlled room conditions. A cooling capacity of 10 kW is fixed to simulate medium refrigeration conditions present in ultralow-temperature rooms. Superheating and subcooling degrees of 5 K and 2 K are selected to propose optimized systems with minimum influence of these parameters.

Table 2. General conditions for the cycle comparison.

Parameter	**Value**
LT evaporating temperature	−80 °C
HT condensing temperature	30 °C
LT cooling capacity	10 kW
LT and HT superheating degree	5 K
LT and HT subcooling degree	2 K

Isenthalpic expansion is assumed in expansion valves present in the circuit. Pressure drops and heat exchange with the ambient in components and lines are neglected.

2.4. Modeling common details

This section presents the common equations used in the modeling process of each cycle configuration.

The refrigerant mass flow rate is calculated using the cooling capacity of the evaporator, Equation (1).

$$\dot{m}_{ref} = \frac{\dot{Q}_{evap}}{(h_{evap,in} - h_{evap,out})} \tag{1}$$

The isentropic efficiency is used to calculate the thermodynamic state at the discharge of the compression stage, Equation (2), which is the ratio between the ideal specific compression work and the real one.

$$h_{disc} = \frac{h_{iso,disc} - h_{suc}}{\eta_{iso}} + h_{suc} \tag{2}$$

Regarding the isentropic efficiency of the compressors, Equation (3) is proposed. It is expressed in terms of compression ratio, Equation (4).

$$\eta_{iso} = -0.0669\,CR^4 + 1.6971\,CR^3 - 15.569\,CR^2 + 57.082\,CR - 0.9003 \tag{3}$$

$$CR = \frac{P_{disc}}{P_{suc}} \tag{4}$$

The compression model is based on manufactured data. Figure 4 shows the validation of the proposed compressor model using manufacturer values and proves the excellent match between both data.

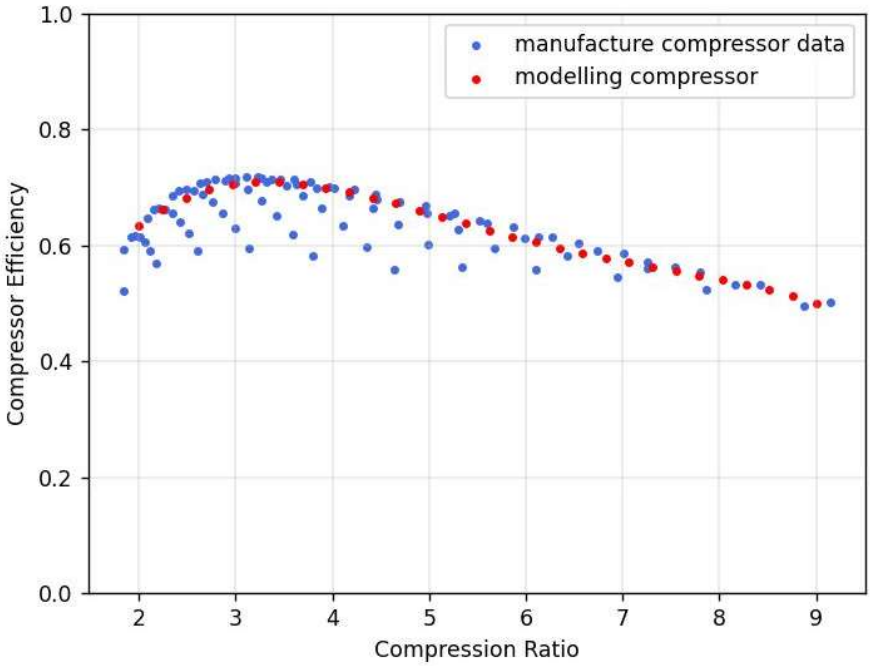

Figure 4. Isentropic efficiency result of compressor modeling and manufacture data

The compressor's power consumption is expressed in Equation (5) as the product of mass flow rate and the real specific compression work.

$$\dot{W}_{comp} = \dot{m}_{comp} \, (h_{disc} - h_{suc}) \tag{5}$$

The total compressor power consumption has been calculated as the sum of all compressors (or compression stages), Equation (6).

$$\dot{W} = \sum \dot{W}_{comp} \tag{6}$$

The coefficient of performance (COP) depends on the cooling capacity and the power consumption, defined as Equation (7).

$$COP = \frac{\dot{Q}_{evap}}{\dot{W}} \tag{7}$$

2.5. Cycles

Considering the common equations presented in the previous subsection, each cycle incorporated in the cascade stages has particular characteristics. Additional equations and remarks for the cycles are exposed in the following, considering the schematics seen in Figure 1.

2.5.1. Single-stage cycle with internal heat exchanger

This cycle has a heat exchanger that receives the refrigerant from the liquid and suction lines, hot and cold sides. Then, the vapor suctioned by the compressor and the liquid before the expansion valve has extra superheating and subcooling, respectively. This heat exchanger is calculated using energy balances considering the hot and cold fluid, Equation (8). The effectiveness of all heat exchangers existing in the configurations is set at 40 % to control excessive discharge temperature [34], Equation (9).

$$\dot{m}_{hot}\left(h_{hot,out} - h_{hot,in}\right) = \dot{m}_{cold}\left(h_{cold,out} - h_{cold,in}\right) \tag{8}$$

$$\varepsilon = \frac{T_{cold,out} - T_{cold,in}}{T_{hot,in} - T_{cold,in}} \tag{9}$$

2.5.2. Vapor and liquid injection two-stage cycles

These cycles (vapor injection and liquid injection) have a mass flow rate at an intermediate pressure, which joins the liquid line with the high-pressure compressor suction line. The intermediate-mass flow rate of the two-stage cycle with liquid injection has been established at 30 % of the evaporator's low-pressure refrigerant mass flow rate. The intermediate flow rate of two-stage cycles with vapor injection has been based on setting the total superheating degree of the high-pressure compressor at 5 K. Required equations come from the energy and mass balance in the pipe joints, Equation (10) and Equation (11).

$$\sum \dot{m}_{in}\, h_{in} = \sum \dot{m}_{out}\, h_{out} \tag{10}$$

$$\sum \dot{m}_{in} = \sum \dot{m}_{out} \tag{11}$$

The intermediate pressure of the compressors in two-stage cycles has been established using Bauman and Blas correlation shown in Equation (12).

$$P_I = \sqrt{P_{evap}\, P_{cond}} \tag{12}$$

2.5.3. Parallel compression with and without economizer

This cycle is based on two compressors, but they work parallel and share the discharge point. Therefore, Equations (10) and (11) are applied before the condenser. A variation of the parallel compression cycle is the addition of a heat exchanger named economizer.

To calculate the necessary mass flow rate through the intermediate line, the economizer effectiveness is set at 80 %. Using the equation for the effectiveness of the heat exchanger, it is possible to determine the necessary mass flow rate and subsequently the enthalpy using an energy balance in the economizer itself. Equation (13) shows the effectiveness, and Equation (14) shows the energy balance.

$$0.8 = \frac{\dot{m}_{il}\,(h_{cold,out} - h_{cold,in})}{\dot{m}_{ref}\,c_p\,(T_{hot,in} - T_{cold,in})} \quad (13)$$

$$\dot{m}_{ref}\left(h_{hot,out} - h_{hot,in}\right) = \dot{m}_{il}\,(h_{cold,in} - h_{cold,out}) \quad (14)$$

2.5.4. Cascade cycle

The modeling of the cascade cycles consists of two different stages but joining them through a cascade heat exchanger. First, the LT condenser temperature is optimized considering the maximum COP. Then, the parameters of the HT evaporator are obtained considering a temperature difference of 5 K between the LT condensing and the HT evaporating temperatures, Equation (15). It is supposed that the HT evaporator absorbs all heat provided by the LT condenser.

$$T_{evap,HT} = T_{cond,LT} - \Delta T \quad (15)$$

2.6. Refrigerants

Two natural refrigerants with appropriate operational and pressure-temperature characteristics are selected for direct cycle comparison: R-170 (ethane) in the LT stage and R-290 (propane) in the HT stage. The thermodynamic states of the refrigerants are incorporated in the simulation software, EES. The working fluids' main properties (physical, chemical, toxicological, and environmental) are included in Table 3.

Table 3. Refrigerants' main properties.

Refrigerant designation	**R-290**	**R-170**
Stage	High	Low
CAS Number	74-98-6	74-84-0
Linear Formula	CH3CH2CH3	CH3CH3
Boiling point	−42.1 °C	−88.6 °C
Critical temperature	96.55 °C	32.17 °C
Critical pressure	4.25 MPa	4.87 MPa
LFL/UFL	1.8 %/8.4 %	1.8 %/8.4 %
ASHRAE Std 34 classification	A3	A3
Auto-ignition temperature	287 °C	287 °C
Molecular weight	44.1 g mol^{-1}	30.1 g mol^{-1}
Heat of combustion	46 MJ kg^{-1}	47 MJ kg^{-1}
Latent heat of vaporization[a]	462.41 kJ kg^{-1}	477.76 kJ kg^{-1}
Vapor density[a]	2.42 kg m^{-3}	2.05 kg m^{-3}
OEL	1000 ppm	1000 ppm
RCL	5300 ppm	7000 ppm
$GWP_{100\text{-}yr}$	<1	5.5
Oil type	AB, MO, POE	AB, MO, POE

[a] at a pressure of 1 atm.

As seen, both refrigerants are highly flammable (A3), and additional measures could be taken, depending on the placement of the system and the final refrigerant charge. Besides, they have a very low GWP, and therefore, they are future-proof natural refrigerants that environmental regulations will not restrict. The boiling temperature ensures that they can be used without entering a vacuum in each stage. The critical temperature allows subcritical operation. The relatively high heat of vaporization enable them to be refrigerants with a considerable expected refrigerating effect. Moreover, they can be used with different commercially available lubricating oils. Figure 5 presents the T-s and P-h diagrams of these refrigerants used in each stage.

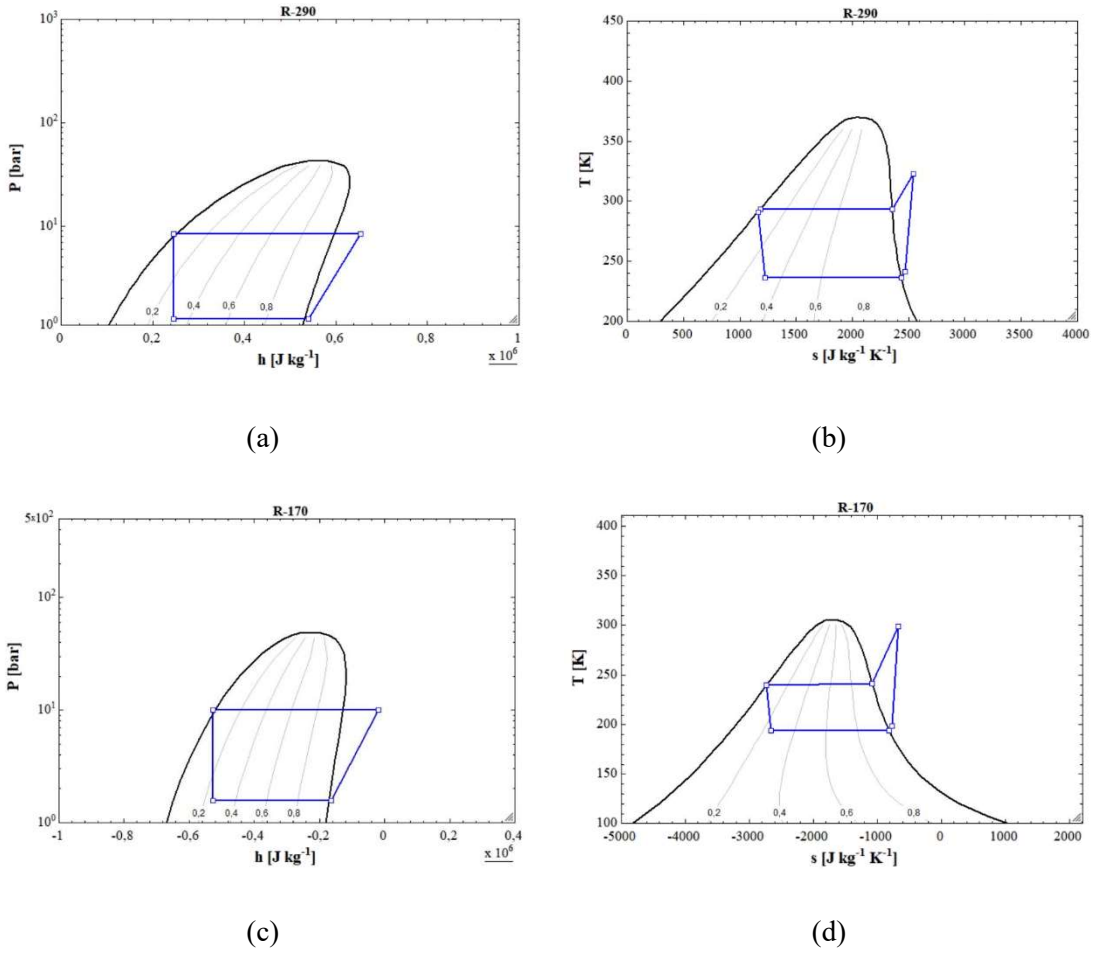

Figure 5. Thermodynamic diagrams: R-290 a) P-h and b) T-s; and R-170, c) P-h and d) T-s.

3. Results

This section presents and analyses the main results of the proposed cycles, focusing on the main parameters of interest from an operational and energetic point of view: coefficient of performance (COP), intermediate temperature, and mass flow rate.

3.1. Coefficient of performance

The COP analysis is divided into subsections according to the primary cycles in which the cascade configuration is based.

3.1.1. Coefficient of performance of base cycles

Figure 6 shows the COP of the cycles considered in this study without combining them in cascades. This can help illustrate the ability of these cycles to cover high-temperature lifts. In this case, a single refrigerant is considered, R-170.

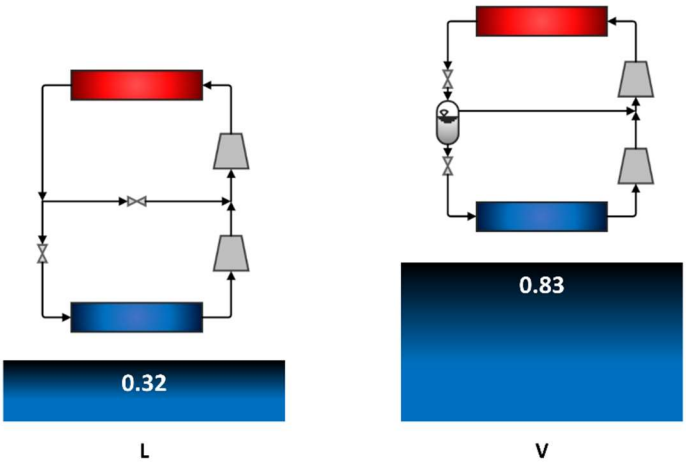

Figure 6: COP of the base cycles.

The use of single-stage cycles for such a high-temperature lift is entirely unfeasible. The compressor cannot compress the very high-pressure lift. Because of that, the pressure lift must be split into more stages. Also, in the case of having a capable compressor, the compressor must absorb a very high amount of energy to compress the refrigerant from suction to discharge pressure for a pressure ratio of 20. This high compression (or pressure) ratio also causes excessive energy consumption. In addition, the discharge temperature is outside the operating range of any compressor (156.5 °C) because there is no intermediate cooling during the compression process. The same happens using an IHX, but the discharge temperature will worsen because of a higher suction temperature.

The two-stage cycle with liquid injection can control the issue of excessive discharge temperatures and compression ratio. The refrigerant is cooled down during the compression stage by introducing liquid from the condenser. Henceforth, this modification makes a COP of 0.32. This low COP is because this cycle forces the refrigerant for ultralow temperatures to work at the higher temperatures for which it is aimed. R-170 has a critical temperature of 32.17 ºC, close to the condenser set of 30 ºC. Therefore, it immediately reaches saturation; the isenthalpic valve places the evaporator inlet at a very high enthalpy, causing an increased mass flow rate that increases the compressor's consumption.

The two-stage cycle with vapor injection can be modeled on two premises: setting the mass flow rate or the superheating degree at the high-pressure compressor suction. For the latter case, the mass flow rate at the intermediate pressure is very high because the enthalpy at this point corresponds to saturated vapor. This causes the mass flow rate through the second compressor to be extremely high, increasing the power consumption (at a constant cooling capacity), so the

COP is reduced. On the other hand, by setting the mass flow rate to pass through that intermediate line, the cooling effect of the vapor is lower but sufficient so that the discharge temperature is no longer out of range. At the same time, the increase in the enthalpy lift of the evaporator has caused the necessary mass flow rate of the cycle to be considerably lower.

Consequently, the necessary energy consumption for the compression is significantly reduced. The total consumption of the compressors has been reduced, causing the COP to be 0.83 for the two-stage cycle with vapor injection. Using the other premise, setting the superheat gives a very low COP as it has a mass flow rate ten times higher. The problem is again the low critical temperature which makes this cycle unfeasible.

The parallel compression is the last configuration used as a reference in the cycle. This way, it is not possible to calculate it because of the same as the single-stage cycles. In this case, a second compressor has a very high-pressure lift and cannot compress it. In the case of using an economizer same occurs.

The single-stage cycle and its successive modifications show that an acceptable COP cannot be obtained. Compressors cannot compress such a high-pressure ratio, and also refrigerants capable of reaching such ultralow temperatures have a low critical temperature.

3.1.2. Coefficient of performance in cascade systems

Figure 7 shows the COPs of the cascade systems in all possible combinations in which parallel compression is not considered. Therefore, sixteen configurations are analyzed in this subsection.

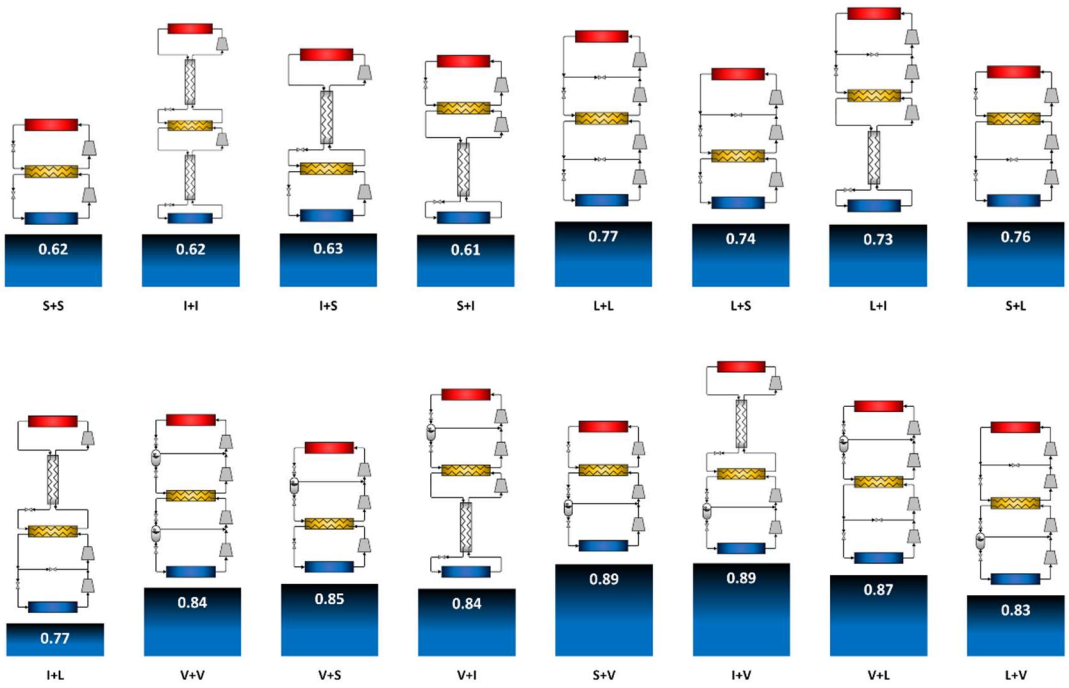

Figure 7. COP of configurations based on cascade systems.

Once the base cycles have been discussed, they can be combined in a cascade. The two-stage cascade cycle based on single-stages, the union of two base cycles, yields a COP of 0.62. The division of the compression process into two compressors explains this significant

improvement, as exposed in the previous section. By dividing into two stages and placing a specific refrigerant to the temperature level, the maximum discharge pressure of each stage is approximately 10 bar. In addition, the effect of the isentropic performance of the compressors also has a substantial influence.

By introducing an IHX in each stage, the COP remains similar, resulting in 0.62. Two two-stage cascade configurations have been modeled, each with the IHX in a different stage (HT or LT), to explore the possible variation of the COP. In both cases, the COP remains similar. The IHX in the HT stage, COP of 0.63, whereas when placed in the LT stage, COP of 0.61.

By separating the compression process and introducing a two-stage cycle with liquid injection in both stages, the COP increase, reaching 0.77. The refrigerant injection explains the increase in the intermediate stage, which allows a lower compression ratio and an increase in performance. To a lesser extent, the internal performance of the compressors also leads to an improvement in COP because the compression slope is less steep. As the cascade reduces the partial compression ratio, dividing each compression ratio again makes the performance increase less noticeable. When the liquid injection is only used in one of the two stages, the COP is similar to or lower than concerning use in both stages. While a two-stage with liquid injection cycle in HT and a single-stage cycle in LT is used, decrease the COP to 0.74, the reverse configuration results in a COP of 0.76. If an IHX is used in the single-stage cycle, more considerable variations can be observed than in the two-stage cascade. The COP decreases when the IHX is placed in the LT single-stage cycle (0.73), whereas it rises in the HT stage, 0.77.

The vapor injection causes the same effect as in the single-stage cycle; it enhances the COP until 0.84 when introduced in both stages. Besides, it causes a greater COP placed only in the LT stage (0.89) than in HT (0.85). A similar COP is observed when an IHX is introduced in the single-stage cycle. In the option with vapor injection in HT and single-stage with IHX in LT, the COP decreases to 0.84. In contrast, in the reverse cycle, the COP remains at 0.89.

At this point, it is necessary to analyze the cycles with vapor injection in HT and also the cycles with liquid injection in HT since the results of the COP of 0.85, 0.84, 0.74, and 0.73 are not the maximum obtained at the optimum temperature point. The problem is that the optimal intermediate temperature would appear below the point with this COP, resulting in 0.9 the ones with vapor injection. The problem is that R-290 is around 0.6 bar at those temperatures, which is not convenient in operational terms. Consequently, the intermediate cascade temperature has been raised manually.

In the same cycle described above, the single-stage cycle can be changed to a two-stage with liquid injection, leaving one stage with vapor injection in HT and liquid injection in LT and another with vapor injection in LT and liquid injection in HT. Both versions offer different COP, being 0.87 and 0.83 each.

3.1.3. Coefficient of performance in cascade systems with parallel compression

Figure 8 shows the COP of the cascade systems with a parallel compression cycle in high or low stages. The remaining combinations (eighteen) are covered by this subsection, reaching 42 configurations studied in this article.

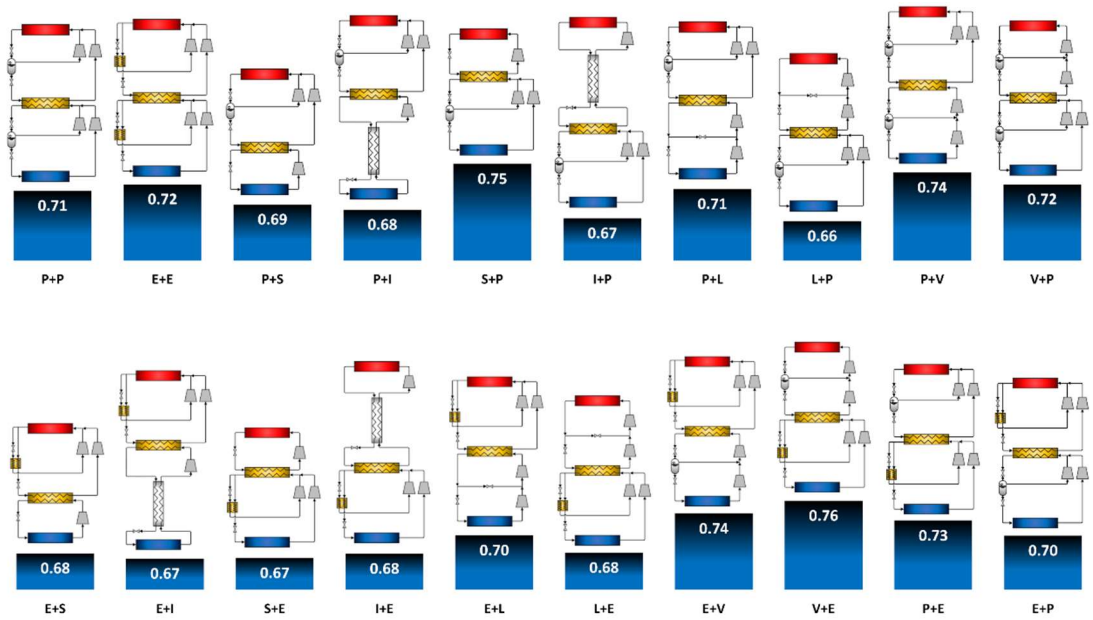

Figure 8. COP of configurations based on parallel compression.

The resulting COP for a parallel compression cycle in both stages is 0.71. By incorporating an economizer, the COP does not vary significantly, 0.72. These results are because the consumption of the second compressor is relatively low due to the cascade cycle. In addition, the parallel compression makes the consumption of the first compressor also low because of the reduced mass flow rate.

This system in parallel compression can, in turn, be combined with the rest of the cycles in a stage. By combining a parallel compression system with a single-stage cycle, the COP is modified depending on cycle configuration. When combining parallel compression in HT and a single-stage cycle in LT, a COP of 0.69 is obtained. If an IHX is introduced, a COP of 0.68 is observed. In the case of placing the reverse, that is, the single-stage cycle in HT, an increase of COP to 0.75 is obtained and when introducing an IHX stays at 0.67.

When replacing the single-stage cycle with a more complex cycle such as the two-stage with liquid injection, a COP of 0.71 is obtained for the parallel compression cycle in HT and liquid injection in LT, while being the reverse, the COP stands at 0.66. On the other hand, adding a vapor injection produces improves each cycle. With a parallel compression cycle in HT and LT two-stage cycle with vapor injection, the COP increases concerning the liquid injection cycle, reaching 0.74. In contrast, a two-stage cycle with vapor injection in HT improves COP to a lesser extent (0.72).

Similar results are observed when changing to an economizer in the parallel compression cycle. In this way, by having a single-stage cycle in LT, the result is 0.68, while in HT is 0.67, and by introducing an IHX, COP keeps in 0.67 and 0.68, respectively.

When replacing the single-stage cycle with a two-stage with liquid injection cycle as in the previous case, a slight increase in the COP is observed, reaching 0.70 with liquid injection in LT. Instead, the liquid injection in HT causes lower COP (0.68), always maintaining the parallel

compression with economizer in the other stage. Finally, when adding a two-stage cycle with vapor injection, in the case of LT, the COP is 0.74 and in HT 0.76.

The last two cycles analyzed are the combination of parallel compression with and without economizer. The parallel compression in HT and parallel compression with economizer in LT results in a COP of 0.73. In the other case, in parallel compression with economizer in HT and parallel compression in LT, COP decreases to 0.70.

3.2. Intermediate temperature

As previously mentioned, the COP of all cycles has been maximized by employing the optimum cascade temperature. Figure 9 shows the values of the optimized LT condensation temperature for all possible combinations studied in this work.

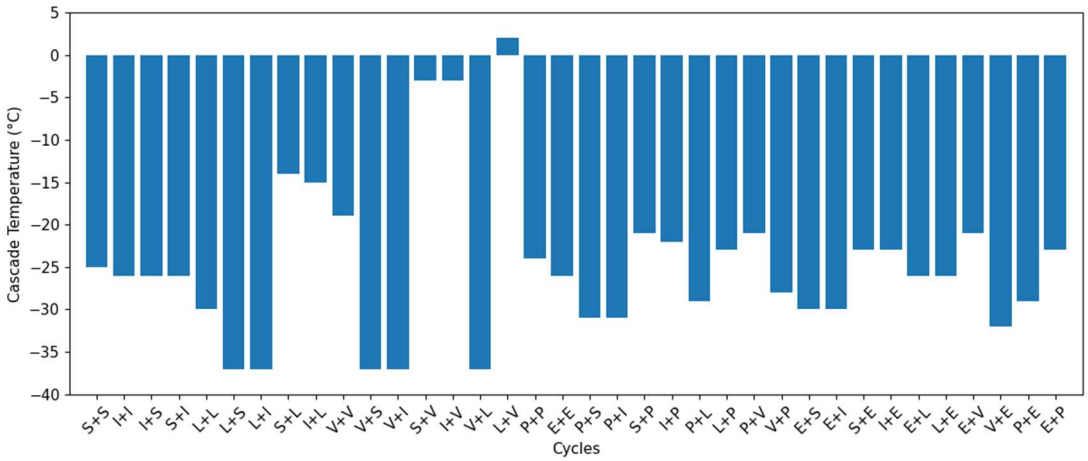

Figure 9. Cascade temperature for all possible combinations.

As can be seen, most configurations have their optimum intermediate temperature roughly midway between condensation and evaporation temperatures. But some cycles have their optimum intermediate temperature closer to the HT condensation or LT evaporation temperatures, as is the case of cycles with a vapor injection. A vapor injection causes a greater temperature lift in the component's stage. This effect occurs both when incorporating it only in HT and only in LT, and it can also be observed that this stage accounts for approximately 75% of the temperature lift. Most of the temperatures of these cycles tend to head towards the opposite side of the vapor injection, becoming somewhat more evident in the case of LT, when cycles like S+V, I+V, or L+V have the optimal cascade temperature closer to 0 ºC. A particularly striking case is the cycle with vapor injection in both HT and LT. In the case of the cycle with vapor injection in both HT and LT, the intermediate temperature is placed approximately in the middle of the total temperature lift, –24 ºC.

3.3. Mass flow rate

Mass flow rate is another essential parameter to analyze the operation of the cycles. In Figure 10, a graph is shown with the mass flow rate results of 38 of the 42 cycles that can be

calculated, considering that the LT cooling capacity required for all configurations is the same, 10 kW.

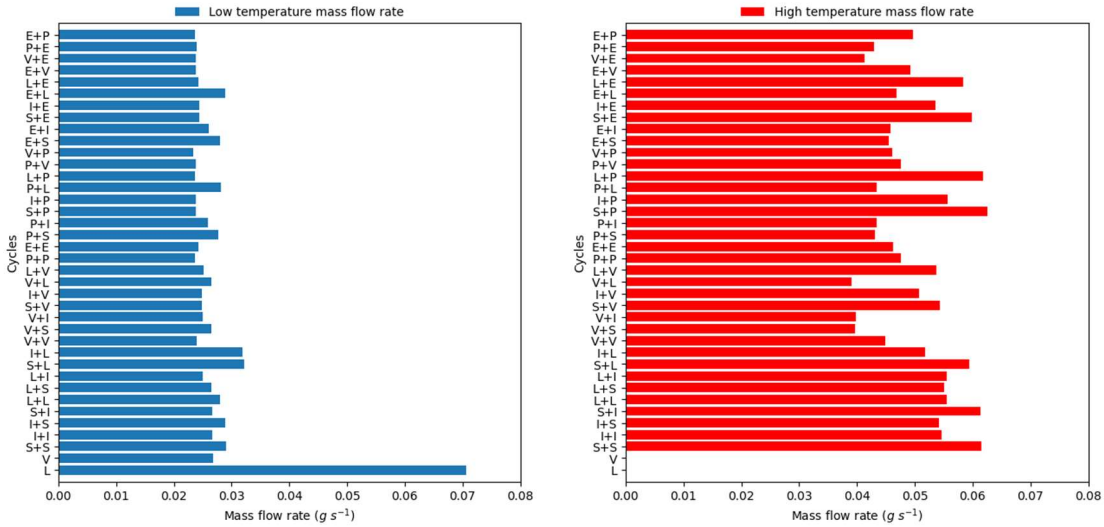

Figure 10. Mass flow rate values for all configurations.

The stages that contain a vapor injection tend to have a lower mass flow rate. Also, the stages that include a single-stage tend to have a higher mass flow rate. Also, the LT stages have a lower mass flow than HT. This is typical of the cascade cycles because the LT condenser power is higher than the evaporator one, so the power of the HT evaporator must be higher and the mass flow rate.

On the other hand, the mass flow rates, including single-stage cycles, are worth mentioning. In the case of cycles with vapor injection, the mass flow rate is minimal because it only has a stage, but it is not viable due to high discharge temperature. The cycle with liquid injection has a very high mass flow rate. This is due to the properties of the refrigerant itself. To reach such low temperatures, it is necessary to use a refrigerant that, on the other hand, does not work at high temperatures. Because of that, R-170 has a critical temperature very close to the 30 ºC of the condenser, making the phase change zone tiny. When adding a vapor injection or a heat exchanger, the increase in the phase change zone is considerable, causing the mass flow to decrease substantially.

4. Conclusions

The lack of studies in ultralow-temperature refrigeration makes this field yet to be optimized and analyzed. However, the sector has not been studied in-depth beyond basic two-stage cascade cycles or three-stage cascades. The operational and energy performance of many cycles have been simulated considering natural refrigerants R-170 and R-290 in the low- and high-temperature stage, respectively. The following conclusions can be summarized.

On the one hand, the need for a minimum two-stage system to obtain acceptable performance is clear, and that two-stage goes through a cascade. This is because by adding more stages, the pressure lift of the compressors is less. Consequently, the COP of the cycles increases because of the compressor efficiency, which is unnecessary in terms of performance. If only a cascade based on single cycles is preferred, an IHX is not a viable option. Incorporating the two-stage cycle with liquid injection causes an increase in the COP that increases even more when incorporating a vapor injection. Also, the two-stage cycle with vapor injection has an interesting performance. Still, the lack of refrigerant capable of working with such a large temperature lift causes very high discharge temperatures and is unacceptable.

Other conclusions related to these technologies are that the vapor injection works better in the LT stage than in the HT stage. The parallel compression cycle is a cycle that improves the results of a single-stage cycle, but is not enough to be considered. In addition, the use of a compressor that must compress the entire stage, being LT or HT, makes it a compressor expected to have a shorter useful life as it has a higher workload than the rest. Another critical aspect is the impossibility of using a parallel compression cycle with an economizer if the temperature lift is very high and requires a refrigerant that cannot work at standard or high temperatures.

To sum up, the cycles with the highest performance are two-stage with vapor injection in LT. Single-stage, single-stage with IHX and two-stage with liquid injection in LT with two-stage with vapor injection in HT offers the highest COP (0.89 and 0.87 the last one), 43.5 % higher with the same refrigerants than a two-stage cascade cycle based on single-stages (COP of 0.62). Parallel compression cycles offer a COP between 20 % and 30 % worse than those mentioned above. Cycles with single-stage with IHX offer similar COP to the single-stage cycles, making the IHX unnecessary.

Future research can study the influence of other refrigerants (pure and mixtures) on the energy and operational performance of the proposed cycles, particularly the most promising ones. Moreover, the energy performance must be validated through measurements in an experimental setup. A multi-parameter evaluation involving exergy, environmental, and economic (or its combination) analyses could enrich and complement the analysis provided in this paper.

Acknowledgments

This scientific publication is part of the R+D+i project PID2020-117865RB-I00, funded by MCIN/AEI/10.13039/501100011033. Adrián Mota-Babiloni acknowledges contract IJC2019-038997-I, funded by MCIN/AEI/10.13039/501100011033.

REFERENCES

[1] ASHRAE. ASHRAE Handbook - Refrigeration (SI Edition). Atlanta, Georgia, US: ASHRAE; 2014.

[2] Training on handling, storing and transporting Pfizer BioNTech COVID-19 Vaccine COMIRNATY® (Tozinameran) n.d. https://www.who.int/publications/m/item/training-

on-handling-storing-and-transporting-pfizer-biontech-covid-19-vaccine-comirnaty-(tozinameran) (accessed September 4, 2021).

[3] Mota-Babiloni A, Mastani Joybari M, Navarro-Esbrí J, Mateu-Royo C, Barragán-Cervera Á, Amat-Albuixech M, et al. Ultralow-temperature refrigeration systems: Configurations and refrigerants to reduce the environmental impact. International Journal of Refrigeration 2020;111:147–58. https://doi.org/10.1016/j.ijrefrig.2019.11.016.

[4] Kasi P, Cheralathan M. Review of cascade refrigeration systems for vaccine storage. Journal of Physics: Conference Series 2021;2054:012041. https://doi.org/10.1088/1742-6596/2054/1/012041.

[5] Udroiu CM, Mota-Babiloni A, Espinós-Estévez C, Navarro-Esbrí J. Energy-Efficient Technologies for Ultra-Low Temperature Refrigeration. In: Howlett RJ, Jain LC, Littlewood JR, Balas MM, editors. Smart and Sustainable Technology for Resilient Cities and Communities, Singapore: Springer Singapore; 2022, p. 309–22. https://doi.org/10.1007/978-981-16-9101-0_22.

[6] Pan M, Zhao H, Liang D, Zhu Y, Liang Y, Bao G. A review of the cascade refrigeration system. Energies (Basel) 2020;13. https://doi.org/10.3390/en13092254.

[7] Mumanachit P, Reindl DT, Nellis GF. Comparative analysis of low temperature industrial refrigeration systems. International Journal of Refrigeration, vol. 35, Elsevier; 2012, p. 1208–21. https://doi.org/10.1016/j.ijrefrig.2012.02.009.

[8] Mateu-Royo C, Arpagaus C, Mota-Babiloni A, Navarro-Esbrí J, Bertsch SS. Advanced high temperature heat pump configurations using low GWP refrigerants for industrial waste heat recovery: A comprehensive study. Energy Conversion and Management 2021;229:113752. https://doi.org/https://doi.org/10.1016/j.enconman.2020.113752.

[9] Chung HS, Jeong HM, Kim YG, Rahadiyan L. Temperature characteristics of cascade refrigeration system by pressure adjustment. Journal of Mechanical Science and Technology 2005;19:2303–11. https://doi.org/10.1007/BF02916471.

[10] Lee TS, Liu CH, Chen TW. Thermodynamic analysis of optimal condensing temperature of cascade-condenser in CO2/NH3 cascade refrigeration systems. International Journal of Refrigeration 2006;29:1100–8. https://doi.org/10.1016/j.ijrefrig.2006.03.003.

[11] Chae JH, Choi JM. Evaluation of the impacts of high stage refrigerant charge on cascade heat pump performance. Renewable Energy 2015;79:66–71. https://doi.org/10.1016/j.renene.2014.07.042.

[12] Deymi-Dashtebayaz M, Sulin A, Ryabova T, Sankina I, Farahnak M, Nazeri R. Energy, exergoeconomic and environmental optimization of a cascade refrigeration system using different low GWP refrigerants. Journal of Environmental Chemical Engineering 2021;9:106473. https://doi.org/https://doi.org/10.1016/j.jece.2021.106473.

[13] Di Nicola G, Giuliani G, Polonara F, Stryjek R. Blends of carbon dioxide and HFCs as working fluids for the low-temperature circuit in cascade refrigerating systems.

International Journal of Refrigeration 2005;28:130–40. https://doi.org/10.1016/j.ijrefrig.2004.06.014.

[14] Bhattacharyya S, Garai A, Sarkar J. Thermodynamic analysis and optimization of a novel N2O-CO2 cascade system for refrigeration and heating. International Journal of Refrigeration 2009;32:1077–84. https://doi.org/10.1016/j.ijrefrig.2008.09.008.

[15] Liu XF, Liu JH, Zhao HL, Zhang QY, Ma JL. Experimental study on a-60 °c cascade refrigerator with dual running mode. Journal of Zhejiang University: Science A 2012;13:375–81. https://doi.org/10.1631/jzus.A1100107.

[16] Dubey AM, Kumar S, Agrawal G Das. Thermodynamic analysis of a transcritical CO2/propylene (R744-R1270) cascade system for cooling and heating applications. Energy Conversion and Management 2014;86:774–83. https://doi.org/10.1016/j.enconman.2014.05.105.

[17] Agnew B, Ameli SM. A finite time analysis of a cascade refrigeration system using alternative refrigerants. Applied Thermal Engineering 2004;24:2557–65. https://doi.org/10.1016/j.applthermaleng.2004.03.013.

[18] Johnson N, Baltrusaitis J, Luyben WL. Design and control of a cryogenic multi-stage compression refrigeration process. Chemical Engineering Research and Design 2017;121:360–7. https://doi.org/10.1016/j.cherd.2017.03.018.

[19] Sun Z, Wang Q, Dai B, Wang M, Xie Z. Options of low Global Warming Potential refrigerant group for a three-stage cascade refrigeration system. International Journal of Refrigeration 2019;100:471–83. https://doi.org/10.1016/j.ijrefrig.2018.12.019.

[20] Walid Faruque M, Hafiz Nabil M, Raihan Uddin M, Monjurul Ehsan M, Salehin S. Thermodynamic assessment of a triple cascade refrigeration system utilizing hydrocarbon refrigerants for ultra-low temperature applications. Energy Conversion and Management: X 2022;14:100207. https://doi.org/https://doi.org/10.1016/j.ecmx.2022.100207.

[21] EUR-Lex - 32014R0517 - EN - EUR-Lex n.d. https://eur-lex.europa.eu/legal-content/EN/TXT/?uri=CELEX%3A32014R0517&qid=1608306002561 (accessed March 28, 2021).

[22] Alberto Dopazo J, Fernández-Seara J, Sieres J, Uhía FJ. Theoretical analysis of a CO2-NH3 cascade refrigeration system for cooling applications at low temperatures. Applied Thermal Engineering 2009;29:1577–83. https://doi.org/10.1016/j.applthermaleng.2008.07.006.

[23] Getu HM, Bansal PK. Thermodynamic analysis of an R744-R717 cascade refrigeration system. International Journal of Refrigeration 2008;31:45–54. https://doi.org/10.1016/j.ijrefrig.2007.06.014.

[24] Eini S, Shahhosseini H, Delgarm N, Lee M, Bahadori A. Multi-objective optimization of a cascade refrigeration system: Exergetic, economic, environmental, and inherent safety

analysis. Applied Thermal Engineering 2016;107:804–17. https://doi.org/10.1016/j.applthermaleng.2016.07.013.

[25] Ust Y, Karakurt AS. Analysis of a Cascade Refrigeration System (CRS) by Using Different Refrigerant Couples Based on the Exergetic Performance Coefficient (EPC) Criterion. Arabian Journal for Science and Engineering 2014;39:8147–56. https://doi.org/10.1007/s13369-014-1335-9.

[26] Turgut MS, Turgut OE. Comparative investigation and multi objective design optimization of R744/R717, R744/R134a and R744/R1234yf cascade rerfigeration systems. Heat and Mass Transfer/Waerme- Und Stoffuebertragung 2019;55:445–65. https://doi.org/10.1007/s00231-018-2435-y.

[27] Sun Z, Liang Y, Liu S, Ji W, Zang R, Liang R, et al. Comparative analysis of thermodynamic performance of a cascade refrigeration system for refrigerant couples R41/R404A and R23/R404A. Applied Energy 2016;184:19–25. https://doi.org/10.1016/j.apenergy.2016.10.014.

[28] Kilicarslan A, Hosoz M. Energy and irreversibility analysis of a cascade refrigeration system for various refrigerant couples. Energy Conversion and Management 2010;51:2947–54. https://doi.org/10.1016/j.enconman.2010.06.037.

[29] Aktemur C, Ozturk IT, Cimsit C. Comparative energy and exergy analysis of a subcritical cascade refrigeration system using low global warming potential refrigerants. Applied Thermal Engineering 2021;184:116254. https://doi.org/10.1016/j.applthermaleng.2020.116254.

[30] Mota-Babiloni A, Mateu-Royo C, Navarro-Esbrí J, Molés F, Amat-Albuixech M, Barragán-Cervera Á. Optimisation of high-temperature heat pump cascades with internal heat exchangers using refrigerants with low global warming potential. Energy 2018;165:1248–58. https://doi.org/10.1016/j.energy.2018.09.188.

[31] Adebayo V, Abid M, Adedeji M, Dagbasi M, Bamisile O. Comparative thermodynamic performance analysis of a cascade refrigeration system with new refrigerants paired with CO2. Applied Thermal Engineering 2021;184:116286. https://doi.org/10.1016/j.applthermaleng.2020.116286.

[32] Rodriguez-Criado JC, Expósito-Carrillo JA, Peris Pérez B, Dominguez-Muñoz F. Experimental performance analysis of a packaged R290 refrigeration unit retrofitted with R170 for ultra-low temperature freezing. International Journal of Refrigeration 2022;134:105–14. https://doi.org/https://doi.org/10.1016/j.ijrefrig.2021.11.015.

[33] Klein S. Engineering Equation Solver n.d.

[34] Mota-Babiloni A, Navarro-Esbrí J, Pascual-Miralles V, Barragán-Cervera Á, Maiorino A. Experimental influence of an internal heat exchanger (IHX) using R513A and R134a in a vapor compression system. Applied Thermal Engineering 2019;147:482–91. https://doi.org/10.1016/J.APPLTHERMALENG.2018.10.092.